A&A 404, 171–185 (2003)
DOI: 10.1051/0004-6361:20030407

Astronomy & Astrophysics

The σ Orionis substellar population*,**

VLT/FORS spectroscopy and 2MASS photometry

D. Barrado y Navascués[1], V. J. S. Béjar[2], R. Mundt[3], E. L. Martín[4], R. Rebolo[2,5], M. R. Zapatero Osorio[1], and C. A. L. Bailer-Jones[3]

[1] Laboratorio de Astrofísica Espacial y Física Fundamental, INTA, PO Box 50727, 28080 Madrid, Spain
[2] Instituto de Astrofísica de Canarias, 38205 La Laguna, Tenerife, Spain
[3] Max-Planck-Institut für Astronomie, Königstuhl 17, 69117 Heidelberg, Germany
[4] Institute of Astronomy. University of Hawaii at Manoa. 2680 Woodlawn Drive, Honolulu, HI 96822, USA
[5] Consejo Superior de Investigaciones Científicas, CSIC, Spain

Received 27 November 2002 / Accepted 12 March 2003

Abstract. VLT/FORS spectroscopy and 2MASS near-infrared photometry, together with previously known data, have been used to establish the membership and the properties of a sample of low-mass candidate members of the σ Orionis cluster with masses spanning from 1 $M_{\odot}$ down to about 0.013 $M_{\odot}$ (i.e., deuterium-burning mass limit). We have observed K-band infrared excess and remarkably intense Hα emission in various cluster members, which, in addition to the previously detected forbidden emision lines and the presence of Li I in absorption at 6708 Å, have allowed us to tentatively classify σ Orionis members as classical or weak-line T Tauri stars and substellar analogs. Variability of the Hα line has been investigated and detected in some objects. Based on the K-band infrared excesses and the intensity of Hα emission, we estimate that the minimum disk frequency of the σ Orionis low-mass population is in the range 5–12%.

Key words. open clusters and associations: individual: σ Orionis – stars: low-mass, brown dwarfs

1. Introduction

This paper is part of a series devoted to the study of the young, nearby open cluster associated with the σ Orionis multiple star (O9.5 V spectral type). The clustering of B stars around σ Orionis was noticed by Garrison (1967), whereas the cluster was listed by Lyngå (1981, 1987) and re-discovered by Wolk (1996) and Walter et al. (1997) using ROSAT data and spectroscopic and photometric follow-up. This stellar association is characterized by its moderate closeness (the Hipparcos distance is $d = 352^{+166}_{-85}$ pc), young age ($\tau = 4.2^{+2.7}_{-1.5}$ Myr by Oliveira et al. 2002. See Zapatero Osorio et al. 2002a for another estimate) and low interstellar reddening ($E(B-V) = 0.05$, Lee 1968; Brown et al. 1994).

So far, we have carried out a census of its population, both stellar and substellar. Substellar objects can be subclassified as brown dwarfs (BDs) and isolated planetary–mass objects (IPMOs). The first type is characterized by the lack of stable hydrogen burning during any stage of their evolution, whereas the second group is unable of any nuclear reaction of energetic significance at all, including the deuterium burning. For solar metallicity, the borderlines have been computed as ~0.075 $M_{\odot}$ and ~0.013 $M_{\odot}$, respectively (Kumar 1963; D'Antona & Mazzitelli 1994, 1997; Saumon et al. 1996; Burrows et al. 1997; Chabrier et al. 2000). The initial searches of substellar components in the σ Orionis cluster were presented in Béjar et al. (1999) and Zapatero Osorio et al. (1999). The discovery of IPMOs in this association, by means of photometric searches and the spectroscopic confirmation of the cool nature of three of them, was presented in Zapatero Osorio et al. (2000), whereas their substellar nature was established via optical and infrared spectroscopy in Martín et al. (2001) and Barrado y Navascués et al. (2001). In this last paper, we presented the first detection of Hα emission in IPMOs. The substellar Initial Mass Function (IMF) of the cluster was derived by Béjar et al. (2001) and binarity was investigated in Martín et al. (2001). In Zapatero Osorio et al. (2002a), we established that the most likely age of the cluster is 3 Myr, and it is effectively bracketed between 1 and 8 Myr, based on the evolution of their eponymous star and the lithium photospheric content of its low mass members. Additionally, we detected Hα emission in most of the very low mass stars and BDs,

Send offprint requests to: D. Barrado y Navascués,
e-mail: barrado@laeff.esa.es

⋆ These observations were collected at the VLT of the European Southern Observatories.

⋆⋆ Table 2 is only available in electronic form at http://www.edpsciences.org

Table 1. Photometric and spectroscopic data for σ Orionis cluster brown dwarf candidates.

Name	Sp. Type	I_c	$(R-I)_c$	(I_c-J)	alpha (J2000.0) delta (^{hms} $^{\circ}$ $'$ $''$)	pW(Hα) (Å)
(1)	(2)	(3)	(4)	(5)	(6)	(7)
S Ori-J053909.9-022814	M5	16.485 0.012	– –	1.93 0.05	05 39 09.9 -02 28 14	<3.3 –
S Ori-J053911.4-023333	M5	16.731 0.011	– –	2.06 0.05	05 39 11.4 -02 33 33	4.7 1.0
S Ori-J053826.1-024041‡	M8	16.96 0.04	2.04 0.06	2.02 0.07	05 38 26.1 -02 40 41	4.0 2.3
S Ori-J053829.0-024847	M6	17.040 0.010	– –	2.18 0.05	05 38 29.0 -02 48 47	– –
S Ori-J053948.1-022914	M7	18.921 0.009	2.24 0.09	2.52 0.05	05 39 48.1 -02 29 14	6.7 1.6
S Ori-J053912.8-022453	M6	19.425 0.008	– –	2.69 0.05	05 39 12.8 -02 24 53	5.2 2.3
S Ori11	M6	16.424 0.008	1.94 0.06	2.12 0.05	05 39 44.3 -02 33 01	10.5 1.5
S Ori13	M5.5	16.410 0.018	1.93 0.06	2.27 0.05	05 38 13.1 -02 24 10	8.1 2.0
S Ori15	M5.5	16.789 0.014	1.81 0.07	2.31 0.05	05 38 48.0 -02 28 54	15.7 2.3
S Ori17[1]	M6	16.945 0.009	1.88 0.06	2.17 0.05	05 39 04.4 -02 38 35	10.9 2.7
S Ori20^{+}	M5.5	17.321 0.009	1.68 0.07	2.42 0.05	05 39 07.4 -02 29 08	3.7 1.0
S Ori22	M6	17.109 0.008	2.11 0.07	2.47 0.05	05 38 35.2 -02 25 24	6.8 3.4
S Ori25[2]	M7.5	17.163 0.008	2.17 0.10	2.46 0.05	05 39 08.8 -02 39 58	41.8 8.5
S Ori26*	M4.5	17.264 0.008	1.83 0.08	2.30 0.05	05 39 16.6 -02 38 27	6.6 3.5
S Ori27[3]	M7	17.08 0.05	2.13 0.07	2.22 0.05	05 38 17.3 -02 40 24	5.1 2.1
S Ori29^{+}[,4]	M6.5	17.230 0.008	1.98 0.07	2.11 0.05	05 38 29.5 -02 25 17	4.2 1.5
S Ori30	M6	17.438 0.008	1.71 0.08	2.19 0.05	05 39 13.0 -02 37 51	16.5 5.5
S Ori31[a]	M7	17.429 0.008	2.03 0.05	2.29 0.05	05 38 20.9 -02 46 13	2.5 0.9
S Ori38	M7	17.640 0.008	2.19 0.09	2.46 0.05	05 39 15.1 -02 21 52	57.4 7.9
S Ori39[5]	M6.5	17.922 0.008	2.24 0.10	2.47 0.05	05 38 32.4 -02 29 58	9.9 3.7
S Ori42	M7.5	19.01 0.09	2.47 0.41	2.33 0.20	05 39 23.3 -02 40 57	88.6 12.5
S Ori44[b,6]	M7	19.39 0.06	2.31 0.15	2.12 0.06	05 38 07.0 -02 43 21	3.3 1.2
S Ori45[7]	M8.5	19.724 0.009	2.75 0.017	2.95 0.05	05 38 25.6 -02 48 36	26.4 15.4
S Ori49*	M7.5	20.83 0.07	>1.5 –	2.22 0.07	05 38 22.9 -02 37 55	4.2 3.7

[a] P(rot) = 7.5 ± 0.6 hours, [b] Undetermined P(rot) (Bailer-Jones et al. 2001).
Spectra types and previous pEW(Hα) from Béjar et al. (1999): [1] M6 and 5.5 Å, [2] M6.5 and 45.0 Å, [3] M7 and 6.1 Å, [4] M6 and 28.0 Å, [5] M6.5 and 5.1 Å, [6] M6.5 and <5 Å, [7] M8.5 and 60.0 Å.
* Probable non-member based on the spectral type classification.
$^{+}$ Probable non-member, Kenyon et al. (2001). Based on a low S/N spectrum.
‡ Photometric binary.

as well as several forbidden lines ([OI]6300 Å, [OI]6364 Å, [NII]6548 Å, [NII]6583 Å, [SII]6716 Å, [SII]6731 Å) in about a third of objects belonging to this sample, indications of accretion and/or mass ejection. Finally, in Zapatero Osorio et al. (2002b) and Barrado y Navascués et al. (2002a), we investigated the presence of very strong Hα emission of unknown origin in two members with masses around the planetary-domain limit (S Ori 55 and S Ori 71).

This paper complements our previous works on Hα emission, focussing on objects with masses around the substellar limits at about 0.075 $M_{\odot}$ and those with masses above the deuterium border at about 0.013 $M_{\odot}$. In the present paper, we derive the spectral types, study the infrared properties and try to disentangle the origin of the detected Hα emission line in a sample of brown dwarfs belonging to the σ Orionis cluster, discussing the possible presence of accretion disks in a fraction of them.

2. Observations

2.1. Red optical spectroscopy

Spectra were collected at the Very Large Telescope Unit #1 on the Paranal Observatory of the European Southern Observatory during 2000, December 23–27. We used the FORS1 spectrograph and the multi-slit capability. FORS1 has a 0.2″/pixel scale in the standard resolution, and yields a field of view of $6.8' \times 6.8'$. We used the 150I grism and the order-blocking filter OG590. With a slit width of 1.4″, the resolution is $R \sim 250$ for the spectral coverage of our data. All of our targets are σ Orionis brown dwarf candidates selected from the surveys of Béjar et al. (1999, 2001), except for a few, which belong to the survey described in Béjar et al. (2003, in preparation). We optimized the multi-slit masks to include as many faint, red candidate members as possible. Individual exposure times were 2400 s. In the particular case of S Ori 13, we only collected data during 1290 s. For S Ori 11, 15, 20, 27, 38, and 39, we obtained a sequence of up to 7 consecutive individual spectra. Table 1 lists magnitudes, optical and infrared colors, as well as the derived spectral types (see Sect. 3.1) and other useful information of our targets.

The data were reduced using standard procedures within the IRAF[1] environment. Additional information on data

[1] IRAF is distributed by National Optical Astronomy Observatories, which is operated by the Association of Universities for Research in Astronomy, Inc., under contract to the National Science Foundation, USA.

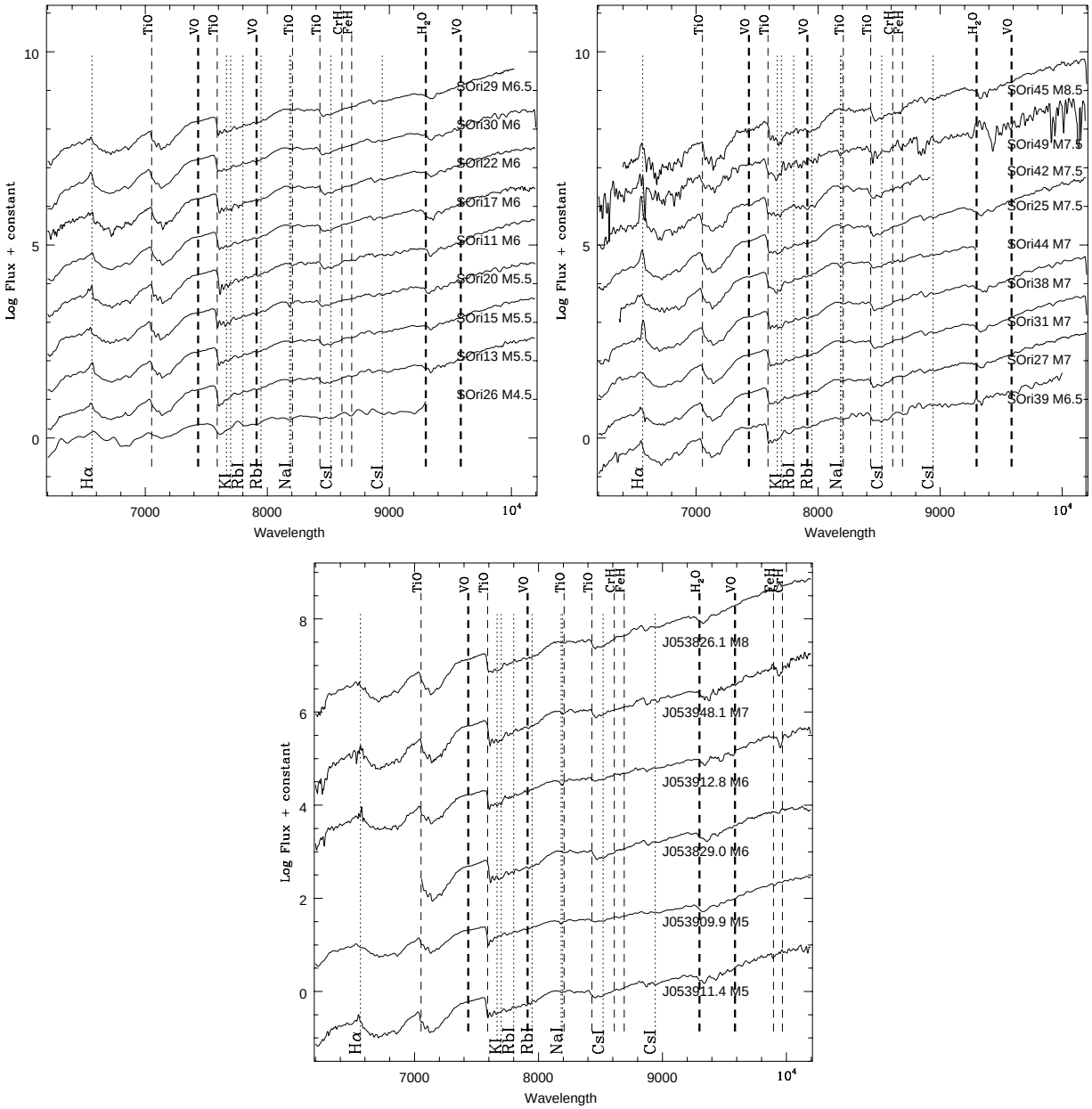

Fig. 1. VLT/FORS spectra of brown dwarf candidate members of the σ Orionis cluster (ordered by decreasing spectral type). Note the logarithmic scale in the flux-axis.

reduction can be found in Barrado y Navascués et al. (2001), where we presented the VLT spectra of many σ Orionis planetary-mass objects. Whenever several exposures were available, the images were added together before the spectrum extraction, producing an average two dimensional spectrum image. Then, in both the average and individual frames, the spectra were extracted using the "apall" algorithm within IRAF. We removed the sky emission lines and background contributions by fitting the sky during the extraction procedure. The wavelength calibration was performed using He Ar Hg Cd comparison arcs taken with the same instrumental configuration. Then, data were flux calibrated using several spectrophotometric standard stars. The final signal-to-noise ratios (S/N), as measured in the 7300–7600 Å region, are in the range 150–20, corresponding to the brightest objects (I = 16.4–17.5) or targets with multiple exposures and to the faintest objects (I = 19.01–20.83) with only one exposure (S Ori 42, 45, and 49). Figure 1 displays the spectra of our σ Orionis brown dwarf candidate members. In addition to the σ Orionis targets and for comparison purposes, we also observed several nearby field objects of M and L spectral types drawn from the lists of Kirkpatrick et al. (1999) and Martín et al. (1999).

2.2. Near-infrared photometry

We also searched the 2MASS point source catalog (Skrutskie et al. 1997), second incremental release, to identify the near-infrared counterparts of σ Orionis low-mass stars and brown dwarfs from our lists of optical sources. We used a searching radius of 5″. The results are listed in Table 2. The offsets

between the optical and infrared coordinates are given in Col. #7, and the coordinates according to the 2MASS catalogue, more accurate than previously published positions, are provided in Col. #8. The 2MASS coordinates are generally within the error bars of the "optical" astrometry. Figure 2 illustrates the optical-near-infrared color-magnitude diagram. 2MASS data are represented with circles (solid circles for objects with VLT spectroscopy presented in this paper); other data taken from Béjar et al. (2001) and Martín et al. (2001) are plotted with the plus and cross symbols, respectively. Error bars (only $-\Delta K$ and $+\Delta(J-K)$ are depicted) are displayed. Three isochrones, corresponding to an age of 3 Myr, and representing non-dusty, dusty and condensed models from the Lyon group (Baraffe et al. 1998; Chabrier et al. 2000) are also displayed in the figure. We remark the peculiar behaviour of the σ Orionis photometric sequence at around $K = 18$ mag, where the $J-K$ color turns to blue values. This effect is supposed to be explained by the settlement of atmospheric dust particles at the bottom of the object's photosphere (see Martín et al. 2001, and references therein).

One object, namely S Ori 47, has *JHK* data coming from United Kingdom infrared telescope (UKIRT). These data were taken under photometric conditions in February 2000.

We have used the following values of cluster distance and interstellar reddening to produce various figures of this paper: $d = 352^{+166}_{-85}$ pc, $E(B-V) = 0.05$ (Lee 1968; Brown et al. 1994), $E(R-I)_c = 0.035$, $E(I_c-J) = 0.049$, $E(I_c-K) = 0.076$, $E(J-K) = 0.027$, $A_V = 0.156$, $A_I = 0.093$, $A_J = 0.044$, and $A_K = 0.017$. Many of these values have been derived from the interstellar extinction law and transformation equations between filters and photometric systems published by Rieke & Lebofsky (1985) and Taylor (1986).

3. Analysis and discussion

3.1. Spectral types

In Fig. 1 we have included the identification of the major atomic and molecular spectroscopic features characteristic of late-M and L spectral classes, like K I λ7665 and λ7699 Å, Na I λ8183 and λ8195 Å, Rb I λ7800 and λ7948 Å, Cs I λ8521 and λ9843 Å, and absorption bands of TiO, FeH, CrH, VO and H_2O. The differences in the slope of the pseudo-continuum and the change in the strength and width of the VO and TiO bands can be appreciated in the VLT spectra of Fig. 1. Kirkpatrick et al. (1999) and Martín et al. (1999) provide a complete summary of the properties of very cool optical spectra of field objects. We can classify our σ Orionis candidates based on their spectroscopic criteria. Flux ratios and spectral indices that account for the pseudo-continuum slope have been measured over the observed VLT data, and we have compared these measurements to those of well-known spectroscopic standard stars to derive spectral types. Our final classification, given in Table 1, ranges from M5 down to M8.5. The uncertainty is estimated at half a subclass. Seven out of the total of 25 VLT objects have also been observed to a higher spectroscopic resolution by Béjar et al. (1999). Their typing, which fully agrees with our classification considering error bars, is included in Table 1.

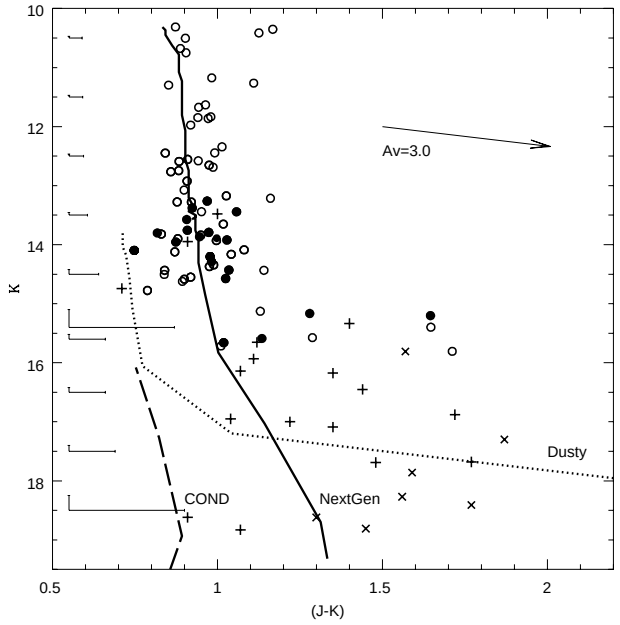

Fig. 2. Infrared photometry for low-mass stars, brown dwarfs and planetary-mass objects of the σ Orionis cluster. Circles correspond to 2MASS data (solid symbols represent data with VLT spectroscopy). Data from Béjar et al. (2001) and Martín et al. (2001) are plotted with crosses and plus symbols, respectively. Models by Chabrier et al. (2000) and Baraffe et al. (1998, 2002) are included in the figure with a thick solid line (dust-free), dotted line (dusty) and long-dashed line (condensed).

3.2. Photometric and spectroscopic membership

Given the very low resolution of our spectra, we cannot obtain accurate radial velocities or see the atomic absorption features due to lithium at 6708 Å and sodium at 8195 Å, which are age-indicators. As discussed in Zapatero Osorio et al. (2002a), all stars and brown dwarfs of the σ Orionis cluster preserve lithium in their atmospheres. Instead, we have combined spectral types and optical and near-infrared photometry to study the cluster membership of our candidates. The Hα emission line, which is also a sign–post of youth, is discussed in Sect. 3.4.

Figure 3 displays I_c magnitudes against spectral types for the σ Orionis cluster, and Figs. 4a and b illustrate the relation between the $(R-I)_c$ and (I_c-J) colors and the spectral classification, respectively. Data from Béjar et al. (1999, 2001), Barrado y Navascués et al. (2001), Martín et al. (2001) and Zapatero Osorio et al. (2002a) are plotted with open circles, whereas the new data of this paper are shown as filled circles. Overplotted is the 3 Myr-isochrone from Baraffe et al. (1998), which provides magnitudes and colors in the filters of interest. This evolutionary isochrone has been converted into spectral type by using the temperature scales of Bessell (1991), Basri et al. (2000), and Luhman (1999). Based on the model, the mass range of the VLT objects spans from the substellar frontier ($0.075\,M_\odot$) down to roughly the planet–brown dwarf boundary ($0.013\,M_\odot$).

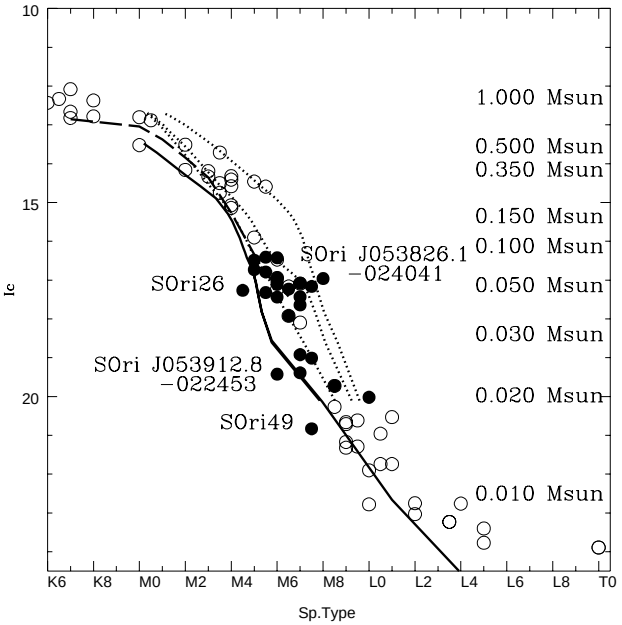

Fig. 3. I_c magnitude against spectral type for the σ Orionis cluster. Solid circles represent data from this study, whereas open circles correspond to data from Barrado y Navascués et al. (2001), Martín et al. (2001), Béjar et al. (2001) and Zapatero Osorio et al. (2002a). The location of the substellar borderline at the cluster age and distance is at around $I_c = 16$ mag. The lines represent several 3 Myr-isochrones from Baraffe et al. (1998), which were obtained for different temperature scales (high gravity by Basri et al. 2000 – solid line; different gravities by Luhman 1999 – dotted lines, and Bessell 1991 – dashed line). Masses are also indicated with the labels in the right hand-side of the diagram.

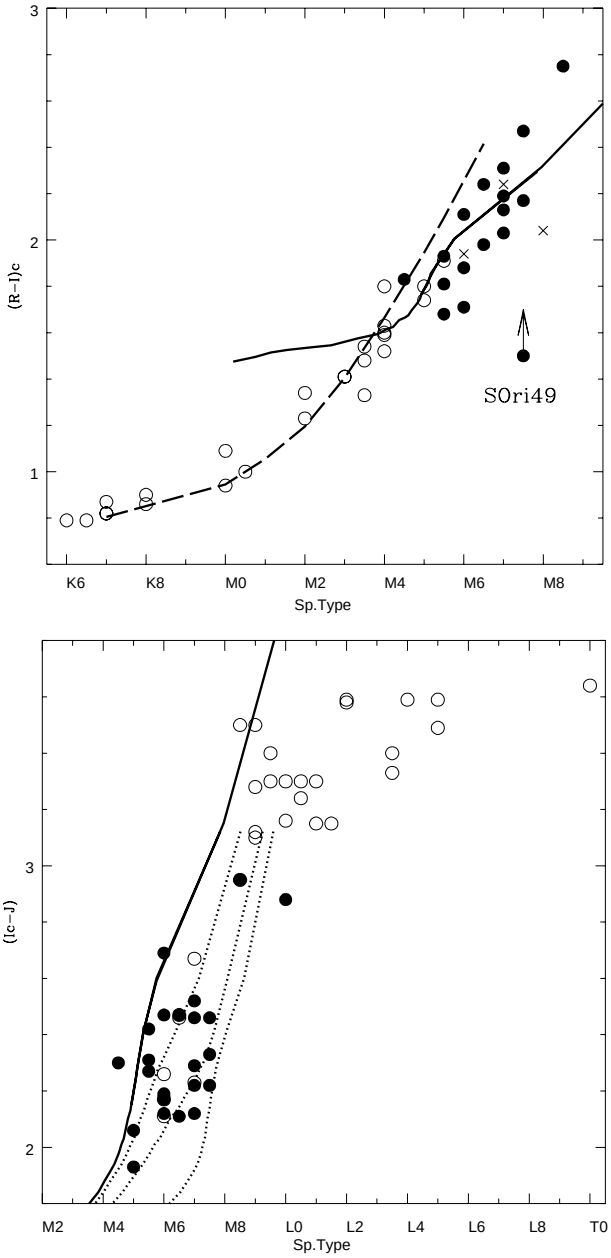

Fig. 4. Spectral type against $(R - I)_c$ color (upper panel) and $(I_c - J)$ color (bottom panel). Solid circles represent data from this paper, whereas open circles correspond to data from Béjar et al. (2001), Martín et al. (2001), Barrado y Navascués et al. (2001) and Zapatero Osorio et al. (2002a). The lines represent several 3 Myr isochrones from Baraffe et al. (1998), which were obtained for different temperature scales (Basri et al. 2000 – solid line, and Bessell 1991 – dashed line, in the upper panel; Basri et al. 2000 – solid lines, and Luhman 1999 – dotted lines in the bottom panel).

These diagrams show a clear continuous sequence of σ Orionis stellar and substellar objects between spectral types K6 and T0. Actually, the cluster spectroscopic sequence extends into the T-class with the finding of S Ori 70, which has been tentatively classified as T6 (Zapatero Osorio et al. 2002c). This object is not included in Figs. 3 and 4b for clarity. Several objects stand out of the cluster sequence, either because they are too faint or too bright for their spectral type, or because their colors do not match the measured spectral type. The objects that are below the sequence are S Ori 49, S Ori 26 and S Ori J053912.8–022453. A possible interpretation for their location in Fig. 3 is that they are spurious members of σ Orionis, cool objects in the neighborhood of the cluster. However, we cannot totally rule out their membership in σ Orionis because these objects may exhibit strong differential reddening, or optical veiling due to accretion from disks (like PC 0025+0447, Martín et al. 1999). This is most likely the case of S Ori J053912.8–022453, since it has significant near-infrared excesses (about $A_V \sim 3$ mag, corresponding to $A_I \sim 1.8$, see Fig. 5). Its de-reddened location in Fig. 3 agrees with S Ori J053912.8–022453 being a true member of the σ Orionis cluster. On the other hand, S Ori 49 and S Ori 26 lack strong Hα emission, a feature that is characteristic of young, cool objects (Sect. 3.4). This may indicate that they are non-members of the cluster. This result agrees with Béjar et al. (2001), who discarded S Ori 49's cluster membership based on the object's near-infrared photometry. Thus, only 2 objects are found to be contaminants among the 25 sources of our sample, i.e., a pollution rate less than 10%.

S Ori J053826.1–024041 (M8) and S Ori 71 (L0) appear quite bright for their spectral types in Fig. 3, which may suggest, apart from the fact that they might be younger than the cluster, that they are binary cluster members (with equal mass components). This situation is similar to that of S Ori 47 (L1,

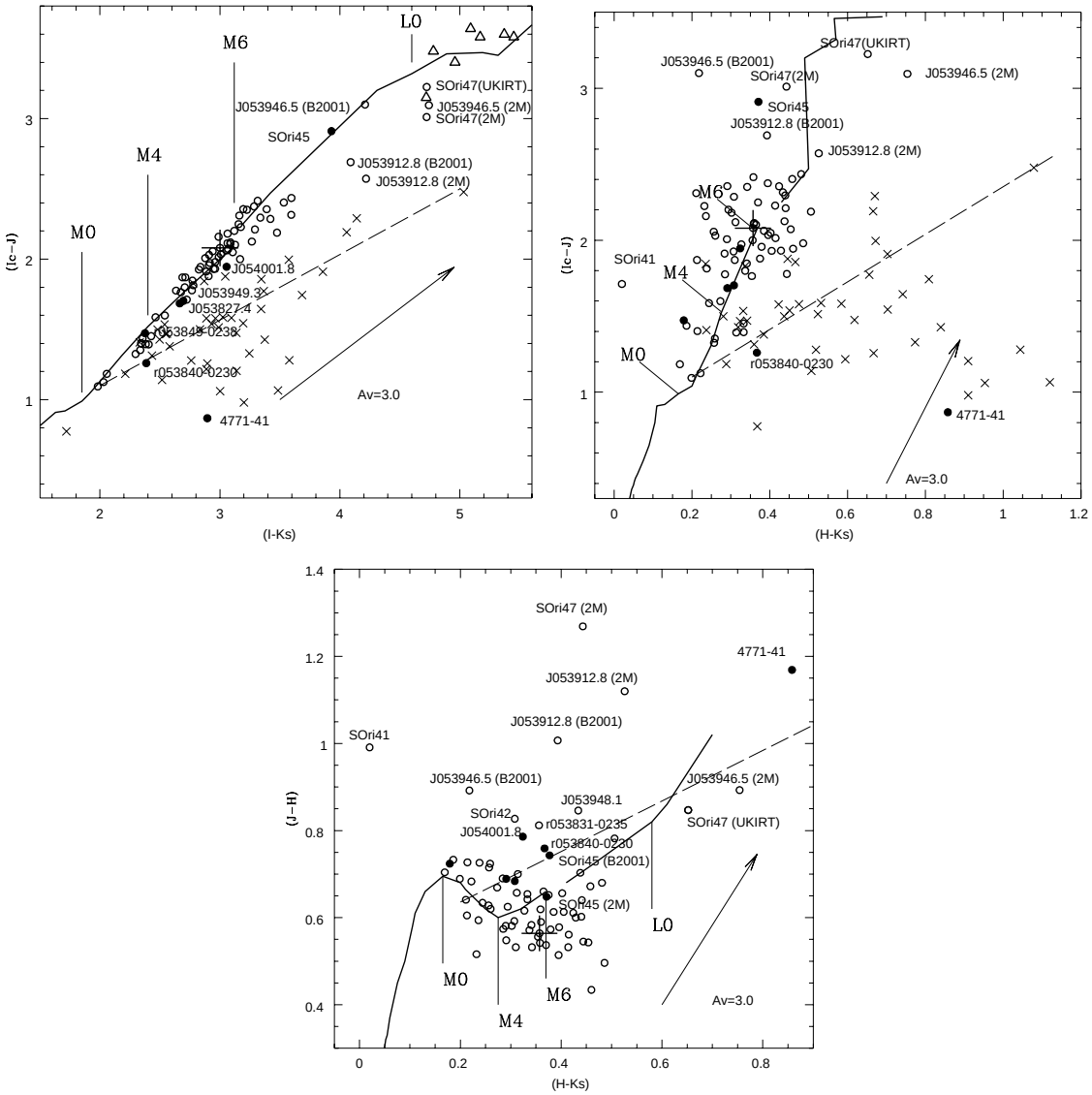

Fig. 5. Optical-Infrared color-color diagrams based on 2MASS data for the σ Orionis population (open circles). Solid circles represent objects with forbidden emision lines. Open triangles correspond to isolate planetary mass objects. Crosses indicate the position of classical T Tauri stars belonging to Orion stellar population (Herbig & Bell 1988). The position of S Ori 12 is indicated with a large plus symbol. The thick-solid and dashed lines correspond to the locii of the main sequence stars (from Bessell & Brett 1988; Kirkpatrick et al. 2000; Leggett et al. 2001) and CTT stars (Meyer et al. 1997 and this paper), respectively.

Zapatero Osorio et al. 1999), a σ Orionis member close to the borderline between brown dwarfs and planetary-mass objects (Barrado y Navascués et al. 2001). The estimated mass of S Ori 71 is also close to the planetary boundary. If the double nature of S Ori 71 and S Ori 47 is finally proved, they would become the first planetary-mass binary systems. S Ori 71 shows an incredibly intense Hα emission. A comprenhensive analysis of this object can be found in Barrado y Navascués et al. (2002a).

3.3. K-band infrared excesses

So far, there is no agreed theoretical mechanism that can satisfactorily explain the formation of brown dwarfs and planetary-mass objects in isolation. See Bodenheimer (1998), Pickett et al. (2000), Boss (2001), Reipurth (2002), Bate (2002), and references therein. The study of infrared excesses, which could be ascribed to the presence of cool "circumstellar" disks, can shed new light on this topic. Figures 5a–c depict the optical and near-infrared color-color diagram of σ Orionis very low-mass stars and brown dwarfs. We note that planetary-mass cluster objects are not included in this discussion because they lack *H*-band photometry (they are too faint to be detected by 2MASS). Stars and brown dwarfs of σ Orionis are displayed as circles (solid circles from those showing forbidden emision lines, Zapatero Osorio et al. 2002a), whereas isolated planetary mass objects appear as open triangles (in this last case, only in panel a). For few objects with large errors in the 2MASS photometry, we have displayed them using *IJK* values from Béjar et al. (2001) and *H* from 2MASS. They are marked in the figures with the labels "2M" and "B2001". As comparison, classical T Tauri stars

from Orion (Herbig & Bell 1998) are displayed as crosses in panel a and b. The main sequence loci (Bessell & Brett 1988; Kirkpatrick et al. 2000; Leggett et al. 2001) and the averaged T Tauri loci (this paper and Meyer et al. 1997) are delineated by solid and dashed lines, respectively. Similar IR color-color diagrams have been obtained by Tej et al. (2002) and Oliveira et al. (2002). These authors conclude that no significant near-infrared excess is evident from the $(J - H)$ versus $(H - K)$ diagram, and that only a fraction of about 6% of the σ Orionis members may be affected by an excess in the K-band. From Fig. 5, and taking into account the spectral types, we infer that at least four objects out of a total of 74 with $IJHK$ photometry, do show an excess at 2.2 μm (namely 4771-41, r053840-0230, S Ori J054001.8 and S Ori 47). Another three might have K excess too, but their 2MASS photometry has quite large uncertainties or their location in some of these diagrams is close to the main sequence loci (i.e., S Ori J053912.8-022453, S Ori J053948.1-022914 and S Ori 42). Thus, based solely on K-band data and assuming that the flux excess is due to the presence of disks surrounding the central object, we derive that the disk frequency among the σ Orionis low-mass population is in the range 5–9%. Note that one object, r053831-0235, has colors (very red) and a spectral type (M0) which indicate that it is strongly reddened. Since it is a probable member of the cluster (it has lithium), this could be due to a small local cloud of dust around the star (in fact, it might have a disk too). If reddened objects are included in the computation, σ Orionis cluster disk frecuency, based on optical and near-IR photometry, increases up to 12%.

However, we remark that disk frequency as measured by K-band excess can be underestimated. Jayawardhana et al. (2002) obtained L' photometry of six very low-mass cluster stars and brown dwarfs and found one object, S Ori 12, with significant L' excess (i.e., 16%). S Ori 12 has a mass estimated at the substellar limit. It does not display a flux excess in the K-band data (as shown in Fig. 5 as a large cross), which suggests that its surrounding disk is neither massive nor warm. It is very likely that a higher fraction of low-mass stars and brown dwarfs of the cluster possesses rather cool "circumstellar" material with signatures that cannot be detected at near-infrared wavelengths. Moreover, Fernández & Comerón (2001), by collecting optical and infrared spectra and photometry of LS-RCrA 1, a star close to the substellar boundary, have shown that an object with very strong emission lines (permitted and forbidden alike) does not have necessarily near infrared excesses at 2.2 microns. On the other hand, disks appear to be common in very young brown dwarfs since many authors have reported evidences on their existence in various star-forming regions (this paper, Muzerolle et al. 2000; Muench et al. 2001; Natta & Testi 2001; Martín et al. 2001; Natta et al. 2002; Jayawardhana et al. 2002; Apai et al. 2002; Testi et al. 2002). In addition, disk frequency among brown dwarfs resembles that of very low-mass stars (Lada et al. 2002). This may indicate that brown dwarfs and low-mass stars share a common origin. However, the precise physical mechanism or mechanisms that give birth to free-floating brown dwarfs and planetary-mass objects remain unknown, although it seems that processes leading to the formation of disks around the central nascent object are more likely.

3.4. Hα 6563 Å and its origin

The equivalent width of the Hα line at λ6563 Å is considered as an age indicator in M-dwarfs, and it is usually associated to stellar activity. In general, the stronger the emission line for a given spectral type, the younger the object. Intense and variable emission characterizes flare stars too (UV Cet type, see Gershberg et al. 1999). Strong Hα emission also appears in episodes of accretion from a close companion in interacting binaries or from a circumstellar disk, as happens in the T Tauri stars and other young stars. In this case, the emission is produced as the accreted material is channeled by magnetic field from the disrupted disk onto the central object (Camenzind 1990), at nearly free-falling velocities.

We have identified Hα in emission in all of the objects listed in Table 1, except in one case (S Ori J053909.9-022814) and have measured the pseudo-equivalent width (pW_λ), since the spectral range around the Hα contains a large number of intense molecular absorption lines. This was carried out using the "splot" task and direct integration within the IRAF environment. The results are listed in column #7 of Table 1. These values correspond to the average emission when several spectra are available. Individual measurements, exposure times and the modified Julian Date (MJD) are listed in Table 3. The spectral range around this feature is shown in Fig. 6, where we have included all the average spectra. Note the very intense emission in the case of S Ori 42, close to 90 Å, and S Ori 38, with 57 Å, and S Ori 25, with about 42 Å.

Figure 7 illustrates the behavior of the Hα feature – equivalent widths – as a function of the spectral type. Solid circles represent the σ Orionis candidate members analyzed in this paper, whereas open circles correspond to members from our previous works in the cluster (Béjar et al. 1999; Barrado y Navascués et al. 2001; Zapatero Osorio et al. 2002a). Plus symbols and crosses represent the location of pre-main sequence (classical T Tauri stars, CTT) and weak-line T Tauri stars (WTT) stars from the Orion population, respectively (Herbig & Bell 1988 and Alcalá et al. 1996). The solid line delimits the areas corresponding to weak-line and classical T Tauri stars. For a comprenhensive discussion of how this criterium was defined, see Barrado y Navascués et al. (2003). Finally, the dotted vertical segments separate the stellar, brown dwarf and planetary-mass domains.

CTT stars are characterized by their emission-line spectrum and non-photospheric continuum excesses, especially in the blue/UV and infrared. Some forbidden emission lines are also present in some cases (see Appenzeller & Mundt 1989 and Bertout 1989 for reviews). On the contrary, WTT stars have spectra typical of main sequence stars, except because the moderate Hα emission and the strong LiI6708 Å doublet in absorption, clear indications of youth. An easy, although not accurate, way of distinguishing whether a star belongs to one or the other category is the Hα equivalent width: larger than 5–20 Å correspond to CTT stars, and smaller to WTT. The actual criterion depends on different authors and the spectral types of the objects. We have chosen a more elaborate criterion, based on data collected in several star forming regions such as Orion, Taurus, Sco-Cen and Chamaeleon (see

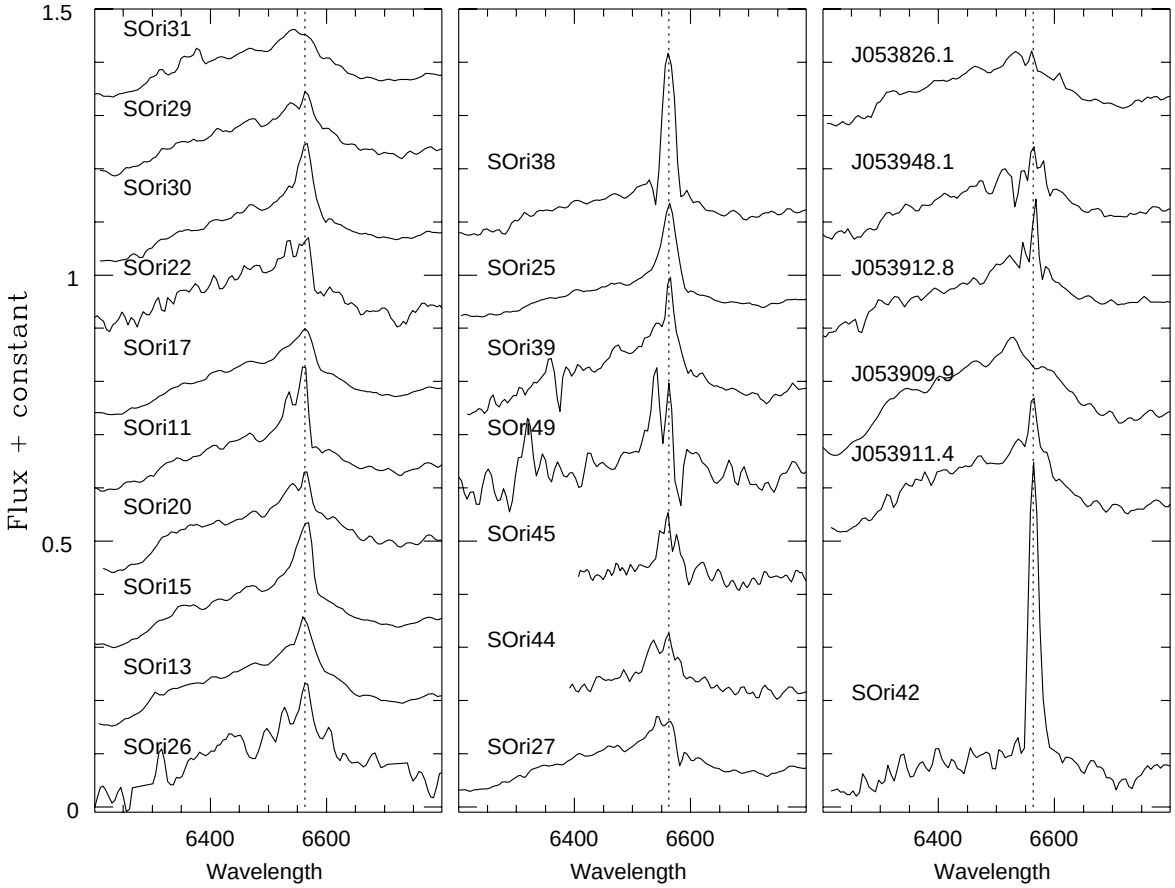

Fig. 6. Details around the Hα line. When several spectra were available, we computed the average, which is the one shown in the figure.

Barrado y Navascués et al. 2003, which discusses an updated version of the quantitative criteria defined in Martín 1997). From the physical point of view, the CTT star features are due to the presence of an accretion disk, which induce, directly or indirectly, the formation of the intense Hα emissions and other emission lines (such as other lines from the Balmer series as well as forbidden lines) and the continuum excesses. The Hα emission is probably produced by the material which is being accreted, whereas the hot continuum comes from the areas where this material hits the central object. The IR excesses correspond to reprocessed energy by the disk (see Sect. 3.3). In some cases there are hot disks which emit large amount of energy at $\sim$2 μm and a significant fraction of the total luminosity comes from the disk. Emission forbidden lines correspond to jets/outflows. Some blue-shifted absorption components of permitted lines are generated by strong winds coming from the inner part of the disk, whereas red-shifted absoptions are direct evidence of infall. In the case of the WTT stars, the disk and all the phenomenology associated to it have disappeared, and the Hα emission is interpreted as enhanced solar-like chromospheric activity induced by rapid rotation. This diagram seems to indicate that there are a population of CTT stars in σ Orionis. In fact, the extrapolation of the WTT/CTT dividing line into the brown dwarf domain suggests that there are substellar counterparts to the CTT stars, or classical T Tauri substellar analogs (CTTSA). Note that, due to its youth, all late spectral type members of the σ Orionis cluster should have lithium. Some

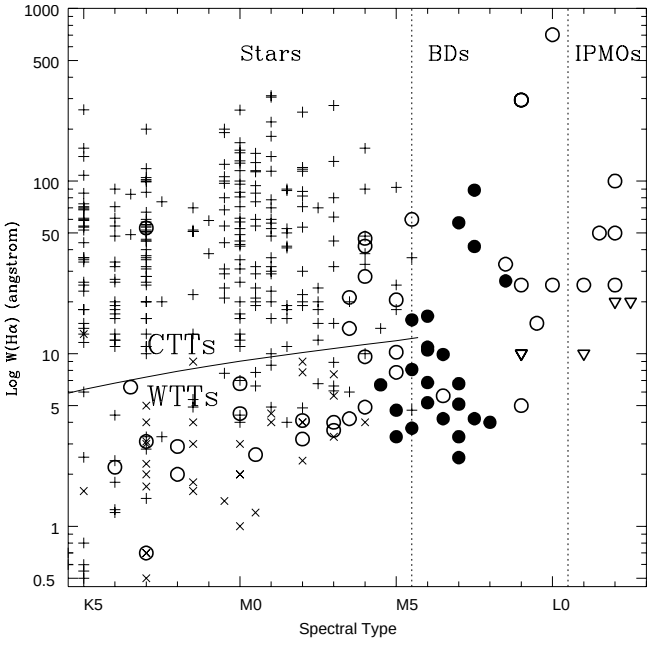

Fig. 7. Hα pseudo-equivalent width versus spectral type. Detections and upper limits in the σ Orionis cluster appear as circles and triangles, respectively. Solid circles correspond to the data of this paper. Open symbols represent data from Béjar et al. (1999), Barrado y Navascués et al. (2001) and Zapatero Osorio et al. (2002a). Crosses correspond to data of pre-main sequence stars of Orion (Herbig & Bell 1988). The solid line separates CTT from WTT stars.

Table 3. Hα equivalent widths and observing dates for the σ Orionis cluster brown dwarf candidates.

name	MJD-51000 (days)	pW(Hα) (Å)	Exp. Time (s)
(1)	(2)	(3)	(4)
S Ori11	904.22764064	12.6 1.5	2400
”	904.26190299	11.0 2.7	2400
”	904.29136284	10.4 2.1	2400
”	904.32053636	10.3 2.1	2400
S Ori13	903.32829829	8.1 2.0	2580
S Ori15	905.13713833	20.8 3.1	2400
”	905.17120378	15.9 3.7	2400
”	905.20057526	15.8 3.5	2400
”	905.23010044	14.0 3.1	2400
”	905.25940527	14.2 2.5	2400
”	905.28869611	17.8 2.9	2400
”	905.31784490	14.2 3.0	2400
S Ori17	904.05650249	10.9 2.7	2400
S Ori20	903.10135488	3.2 0.9	2400
”	903.14482793	2.9 0.8	2400
”	903.17441719	3.3 1.2	2400
S Ori22	905.06892540	6.8 3.4	4800
S Ori25	904.05650249	41.8 8.5	2400
S Ori26	904.05650249	6.6 3.5	2400
S Ori27	903.05138618	5.5 3.1	2400
”	906.03996572	7.3 4.2	2400
”	906.07400201	6.8 3.3	2400
”	906.11072522	4.5 2.2	2400
”	906.14487566	4.6 2.7	2400
”	906.17892987	5.0 3.5	2400
S Ori29	905.06892540	4.2 1.5	4800
S Ori30	904.05650249	16.5 5.5	2400
S Ori31	903.23775122	2.5 0.9	4800
S Ori38	904.12669251	49.0 6.0	2400
”	904.15630248	46.1 8.5	2400
”	904.19053588	49.0 6.4	2400
S Ori39	905.13713833	8.5 3.2	2400
”	905.17120378	8.6 2.9	2400
”	905.20057526	10.1 3.0	2400
”	905.23010044	17.9 3.2	2400
”	905.25940527	11.5 3.9	2400
”	905.28869611	6.0 3.3	2400
”	905.31784490	9.8 5.0	2400
S Ori42	904.05650249	88.3 12.5	2400
S Ori44	903.23775122	3.3 1.2	4800
S Ori45	903.23775122	26.4 15.4	4800
S Ori49	906.11072522	4.2 3.7	4800
S Ori-J053826.1-024041	903.05138618	3.3 1.2	2400
”	906.03996572	6.1 2.2	2400
”	906.07400201	3.7 2.1	2400
”	906.11072522	7.8 2.9	2400
”	906.14487566	1.9 0.7	2400
”	906.17892987	1.3 0.7	2400
S Ori-J053909.9-022814	903.10135488	<0.0 –	2400
”	903.14482793	<0.0 –	2400
”	903.17441719	<0.0 –	2400
S Ori-J053911.4-023333	903.10135488	5.3 1.2	2400
”	903.14482793	4.9 0.8	2400
”	903.17441719	5.4 1.5	2400
S Ori-J053912.8-022453	904.12669251	2.5 0.7	2400
”	904.15630248	1.6 0.9	2400
”	904.19053588	2.8 1.3	2400
S Ori-J053948.1-022914	904.22764064	6.2 3.6	2400
”	904.26190299	4.8 3.5	2400
”	904.29136284	9.1 4.1	2400
”	904.32053636	6.5 4.3	2400

measurements have been obtained by Zapatero Osorio et al. (2002a).

Figure 8 is similar to Fig. 7. In this case, we only plot σ Orionis data (crosses and open triangles for upper limits). Overlapping solid circles indicate those objects from Zapatero Osorio et al. (2002a) which have forbidden emission lines,

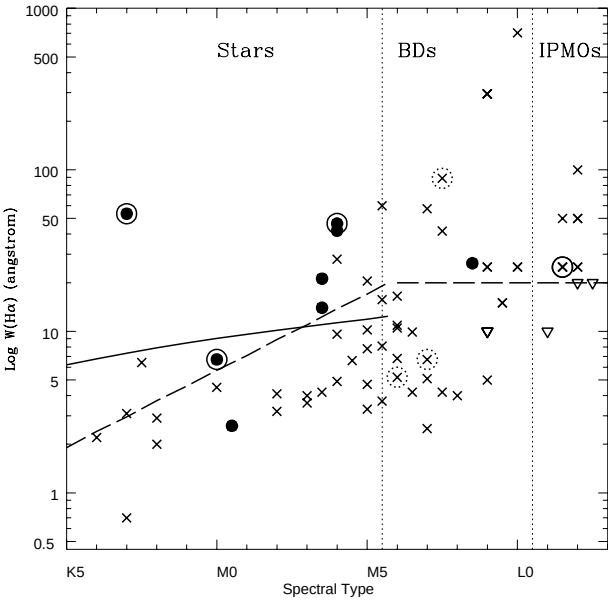

Fig. 8. Hα pseudo-equivalent width versus spectral type for σ Orionis low-mass members. Crosses and open triangles correspond to data from this work, Barrado y Navascués et al. (2001), Béjar et al. (1999) and Zapatero Osorio et al. (2002a) – triangles denote the position of upper limits. Overlapping solid circles stand for objects with forbidden emission lines (Zapatero Osorio et al. 2002a), whereas large open circle discriminate those cluster members with near-infrared excesses. Broken open circles denote possible near-infrared excesses. The solid line separates CTT from WTT stars, whereas the long dashed line correspond to the upper envelope to atmospheric activity (see text).

whereas large open circles discriminate those members which have IR excesses in the K band. The solid line is the dividing line between WTT and CTT stars, whereas the long-dashed line represents the maximum Hα equivalent width due to chromospheric activity (derived using data from young clusters such as IC2391, Alpha Per and the Pleiades. See Barrado y Navascués et al. 2003 for details). This last curve indicates that most of the σ Orionis stellar and substellar population have pW_λ(Hα) in agreement with chromospheric origin. However, some of them show a large emission, which might have different source. We emphasize that only the medium resolution spectra of low mass stars and BDs, discussed in Zapatero Osorio et al. (2002a), are good enough to detect the forbidden lines, and that these lines are not always present in CTT stars. The diagram shows a trend between the detection of these lines, the presence of IR excesses and strong Hα emission measured at this spectral resolution. These three phenomena indicate that, at least, there are a handful of CTT stars and substellar classical T Tauri analogs in the σ Orionis cluster. Moreover, as stated before, the VLT spectroscopic data have a low resolution which cannot allow the detection of emission lines with few Å, typical of forbidden lines which sometimes appear in the spectrum of CTT stars. However, in the literature, the detection of lithium and the Hα emission have been extensively used as criteria to catalog young stars as either CTT or WTT stars. Therefore, we can assume that some substellar objects can be tentatively classified as classical T Tauri analogs.

Table 4 summarized all the available information known so far for low mass stars and BDs of the σ Orionis cluster.

Table 4. Spectral properties and classification of low mass stars and BDs of σ Orionis. We only list those members which have been observed spectroscopically.

Name	MK	K band excess	Hα^{*}	Forbidden lines	Lithium	Type
r053820-0234	M4	N/A	above	N	Y	CTT-
S Ori25	M7.5	N	above	N/A	N/A	CTT-
S Ori38	M7	N	above	N/A	N/A	CTT-
S Ori40	M7	N	above	N/A	N/A	CTT-
S Ori66	L3.5	N	above	N/A	N/A	CTT-
S Ori71‡	L0	N/A	above	N/A	N/A	CTT-
S OriJ053951.6-022248	M5.5	N	above	N	Y	CTT-
S OriJ054005.1-023052	M5	N	above	N	Y	CTT-
S Ori12†	M6	Y	below	N/A	N/A	CTT?
S Ori47 (UKIRT)	L1.5	Y	N/A	N/A	N/A	CTT?
S Ori42	M7.5	Y?	above	N/A	N/A	CTT??
S OriJ053912.8-022453	M6	Y?	N/A	N/A	N/A	CTT??
S OriJ053948.1-022914	M7	Y?	N/A	N/A	N/A	CTT??
4771-41	K7	Y	above	Y	Y	CTT+
r053833-0236	M3.5	N/A	below	Y	Y	CTT+
r053840-0230	M0	Y	below	Y	Y	CTT+
r053849-0238	M0.5	N	below	Y	Y	CTT+
S Ori45	M8.5	N	above	Y	Y	CTT+
S OriJ053827.4-023504	M3.5	N	above	Y	Y	CTT+
S OriJ053949.3-022346	M4	N	above	Y	Y	CTT+
S OriJ054001.8-022133	M4	Y	above	Y	Y	CTT+
S Ori26	M4.5	N/A	below	N/A	N/A	NM?
S Ori49	M7.5	N/A	below	N/A	N/A	NM?
4771-1038	K8	N	below	N	Y	WTT
4771-1051	K7.5	N/A	below	N	Y	WTT
4771-1075	K7	N	below	N	Y	WTT
4771-1097	K6	N/A	below	N	Y	WTT
4771-899	K7	N	below	N	Y	WTT
r053831-0235**	M0	Y	below	N	Y	WTT
r053838-0236	K8	N	below	N	Y	WTT
r053907-0228	M3	N	below	N	Y	WTT
r053923-0233	M2	N	below	N	Y	WTT
S Ori27	M7	N	below	N	Y	WTT
S OriJ053715.1-024202	M4	N	below	N	Y	WTT
S OriJ053820.1-023802	M4	N	below	N	Y	WTT
S OriJ053847.5-022711	M5	N	below	N	Y	WTT
S OriJ053914.5-022834	M3.5	N	below	N	Y	WTT
S OriJ053920.5-022737	M2	N	below	N	Y	WTT
S OriJ053958.1-022619	M3	N	below	N	Y	WTT
S Ori11	M6	N	below	N/A	N/A	WTT?
S Ori13	M5.5	N	below	N/A	N/A	WTT?
S Ori15	M5.5	N	below	N/A	N/A	WTT?
S Ori17	M6	N	below	N/A	N/A	WTT?
S Ori20	M5.5	N	below	N/A	N/A	WTT?
S Ori22	M6	N/A	below	N/A	N/A	WTT?
S Ori29	M6.5	N	below	N/A	N/A	WTT?
S Ori30	M6	N	below	N/A	N/A	WTT?
S Ori31	M7	N	below	N/A	N/A	WTT?
S Ori39	M6.5	N	below	N/A	N/A	WTT?
S Ori44	M7	N/A	below	N/A	N/A	WTT?
S OriJ053826.1-024041	M8	N	below	N/A	N/A	WTT?
S OriJ053829.0-024847	M6	N	below	N/A	N/A	WTT?
S OriJ053909.9-022814	M5	N	below	N/A	N/A	WTT?
S OriJ053911.4-023333	M5	N	below	N/A	N/A	WTT?

* W(Hα) above or below the criteria defined in the text (see Barrado y Navascués et al. 2003).
** Large reddening.
† ($K - L'$) excess from Jayawardhana et al. (2002).
‡ Asymmetry in Hα, Barrado y Navascués et al. (2002a).
CTT+ = Probable Classical T Tauri star or analog, based on forbidden emission lines.
CTT- = Possible Classical T Tauri star or analog, based on Hα.
CTT? = Possible Classical T Tauri star or analog, based on the IR excesses.
CTT?? = Possible Classical T Tauri star or analog? based on possible IR excesses.
WTT = Weak-line TTauri star or analog based, on lithium and Hα.
WTT? = Possible Weak-line T Tauri star or analog, based on Hα.
NM? = Non-member?.
N/A = Data no available.

Column #3 indicates whether the object has IR excess (based on optical and *JHK* 2MASS data). Column #4 states whether the pW_λ(Hα) is above or below the dividing lines between CTT and WTT stars and the upper limit of chromospheric activity (see Fig. 8). Column #5 contains information regarding the presence of forbidden lines, whereas Col. #6 lists the detection of LiI6708 Å, when available. Finally, our classification as classical or weak-line T Tauri stellar (or substellar analog) is shown in Col. #7. This classification was carried out in a hierarchical order and attending to the following scheme:
i) Those members with forbidden lines have been catalogued as probable CTT, and flagged in the table with "CTT+".
ii) Four objects present probable K excess ("CTT?" flag).
iii) Three BDs have possible IR excesses, although the 2MASS errors are large or their location is close to the main sequence loci in some color-color diagram ("CTT??" flag).
iv) Those objects with intense Hα emission are possible classical T Tauri stars or substellar analogs ("CTT-" flag). In some cases, lithium has been detected. In others, its presence is assumed due to the confirmed membership and the age of the cluster (1–8 Myr, Zapatero Osorio et al. 2002a).
v) Whenever lithium has been detected and the object displays a moderate Hα emission (below the criteria defined previously), we have catalogued it as weak-line T Tauri star or substellar analog ("WTT" label).
vi) Finally, σ Orionis members with moderate Hα emission and unknown lithium (due to the low resolution spectroscopy) appear as possible weak-line T Tauri stars or analogs. Note that the lack or an uncertain of detection of IR excess (or forbidden lines) does not mean that they are not present, since additional IR photometry in the 1–5 μm range and/or optical spectroscopy (better at higher resolution) with improved signal–to–noise ration might provide positive detections in some cases. An example is represented by S Ori 47. The 2MASS data indicate that this BD close to the planetary domain and discussed deeply in Zapatero Osorio et al. (1999) and Barrado y Navascués et al. (2001), might have an infrared excess. In this case, 2MASS errors are quite large. Our UKIRT data corresponding to S Ori 47, more accurate than the 2MASS values, indicate that the disk is likely present.

Oliveira et al. (2002), by studying optical and infrared data of σ Orionis candidates, were not able to detect infrared excesses, which also characterized the presence of gas-dusty disks around stellar and substellar objects. However, they do not provide a list with the results or the names of the objects, and we were not able to cross-correlate their results with our BDs. On the contrary, Muench et al. (2001) have been able to detect some evidences for circumstellar disks around BDs, down to 0.02 solar masses, in the Trapezium cluster (~1 Myr), by measuring infrared excesses in about 65% of the sample. Therefore, until further evidence is collected (via higher signal–to–noise, higher resolution spectra), these data seem to indicate that the Hα weak emission comes from the photosphere of the objects, and could be analogous to activity present in late spectral type stars due to the chromosphere, except in a handful of the σ Orionis BDs, which show large equivalent widths, where the origin might be related to accretion.

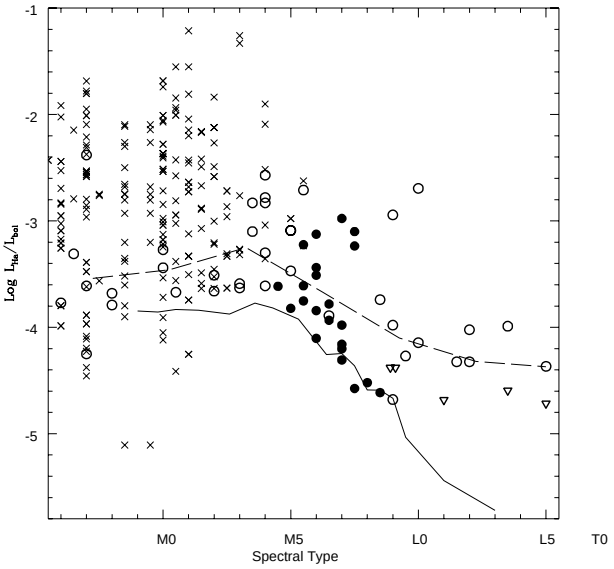

Fig. 9. Ratio between the Hα and bolometric luminosities against spectral type. Data for the Orion pre-main sequence population are shown with crosses, whereas circles and triangles (upper limits) represent σ Orionis members. The solid and long-dashed lines indicate the average locus of field stars (after Hawley et al. 1996 and Gizis et al. 2000) and σ Orionis objects, respectively.

Figures 7 and 8 clearly show that the Hα emission tends to be larger for cooler objects. In the case of the PMS Orion population from the catalog by Herbig & Bell (1988), there is a large increase in the strength at about K0 spectral type. In the case of σ Orionis cluster members, the change in the behavior appears at about M3.5 spectral type (except in one case, 4771-41, a K7 star with large infrared excesses and characterized by forbidden lines, Zapatero Osorio et al. 2002a), when they are fully convective. Note, however, that part of this increase might be due to the strengthening of TiO bands which deplete the continuum, and, therefore, enhance the Hα equivalent width. This increase might not be due to the flux drop in the continuum in cooler objects. In any case, a large range of values is present for a given spectral type in both groups.

We detect intense emission lines even for very low mass objects, such as in the case of S Ori 55, which has a mass ~12 $M_{\rm jupiter}$ and variable Hα emission, with pW_λ(Hα) between 185 and 410 Å (Zapatero Osorio et al. 2002b), and 5 Å (Barrado y Navascués et al. 2001). Another object with a mass close to 20 $M_{\rm jupiter}$, S Ori 71, has the second largest emission ever detected, as far as we know, in a star or BD, with pW_λ(Hα) = 705 Å (Barrado y Navascués et al. 2002a; Luhman et al. 2003). This spectral feature seems to be asymmetric and very broad. The source of these emissions is not clear.

One of the aims of the present paper is to try to establish the origin of the Hα emission seen in most of the σ Orionis low mass members (stars, BDs and IPMOs). In this context, it is important to know how important is for the object the amount of energy release throughout the line. We have computed the ratio between the Hα luminosity ($L_{\rm H\alpha}$) to the bolometric luminosity ($L_{\rm bol}$). The $L_{\rm H\alpha}$ and $L_{\rm bol}$ values were computed following Herbst & Miller (1989) and Hodgkin et al. (1995). See Zapatero Osorio et al. (2002a) for details. Figure 9

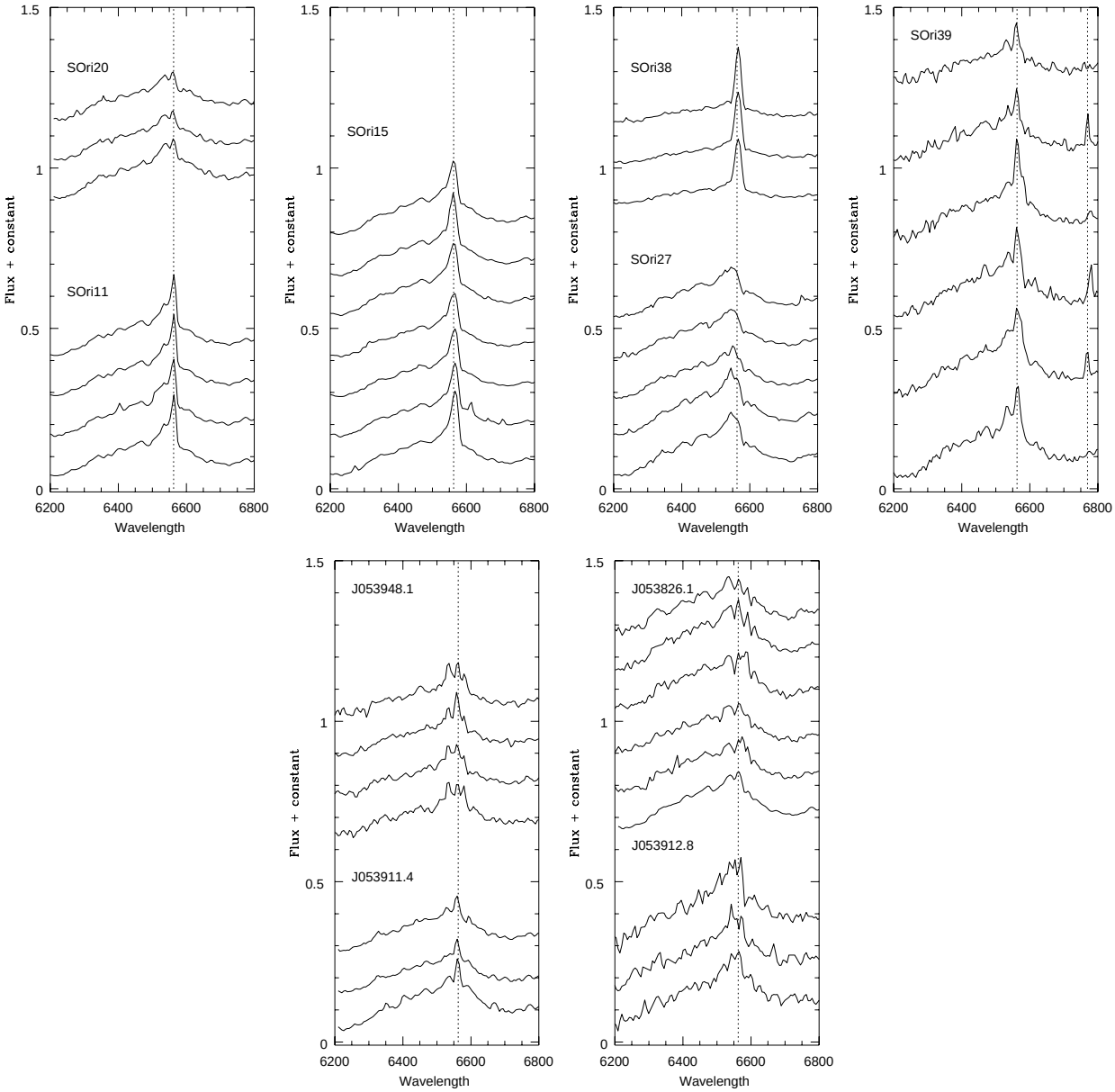

Fig. 10. Individual VLT spectra showing in detail the area around the Hα line.

displays the ratio between $L_{\mathrm{H}\alpha}$ to L_{bol}, versus the derived spectral type. Members of the σ Orionis cluster are shown as open and solid circles, as in Figs. 3 and 4. The average locus for field stars and BDs is plotted as a solid line, whereas the average ratio for σ Orionis members is displayed as a long-dashed line. Clearly, most the of σ Orionis members have ratios higher or much higher than field objects. In fact, most of the isolated planetary-mass objects and about half of the BDs of the σ Orionis cluster have ratios about one order of magnitude larger than their field objects counterparts. Note, however, that field objects are much older and have larger masses. For example, M5 and L0 from the field have masses of 0.090 $M_{\odot}$ and 0.040 $M_{\odot}$ for an age of 100 Myr, 0.110 $M_{\odot}$ and 0.075 $M_{\odot}$ for an age of 1 Gyr, whereas the same spectral types would have 0.070 $M_{\odot}$ and 0.014 $M_{\odot}$ for 3 Myr, the most likely age for σ Orionis cluster (Zapatero Osorio et al. 2002a). In any case, some of the cluster members have ratios close to the saturation limit which appear in active late spectral type stars (see, for instance, Stauffer et al. 1997).

3.5. Hα variability

In addition to the large range of Hα emission for a given spectral type, we have detected variability (the most conspicuous cases being S Ori J053826.1-024041 and S Ori 39). This variability agrees with the WTT star classification for these objects, since it means that its origin would be coronal/chromospheric and, therefore, intrinsically variable. Note, however, that CTT stars have Hα variability too, but in a larger time span or with sudden, un-modulated changes. Figure 10 shows the sequences of spectra around this feature for several objects belonging to our target list. Although uncertainties are large for most

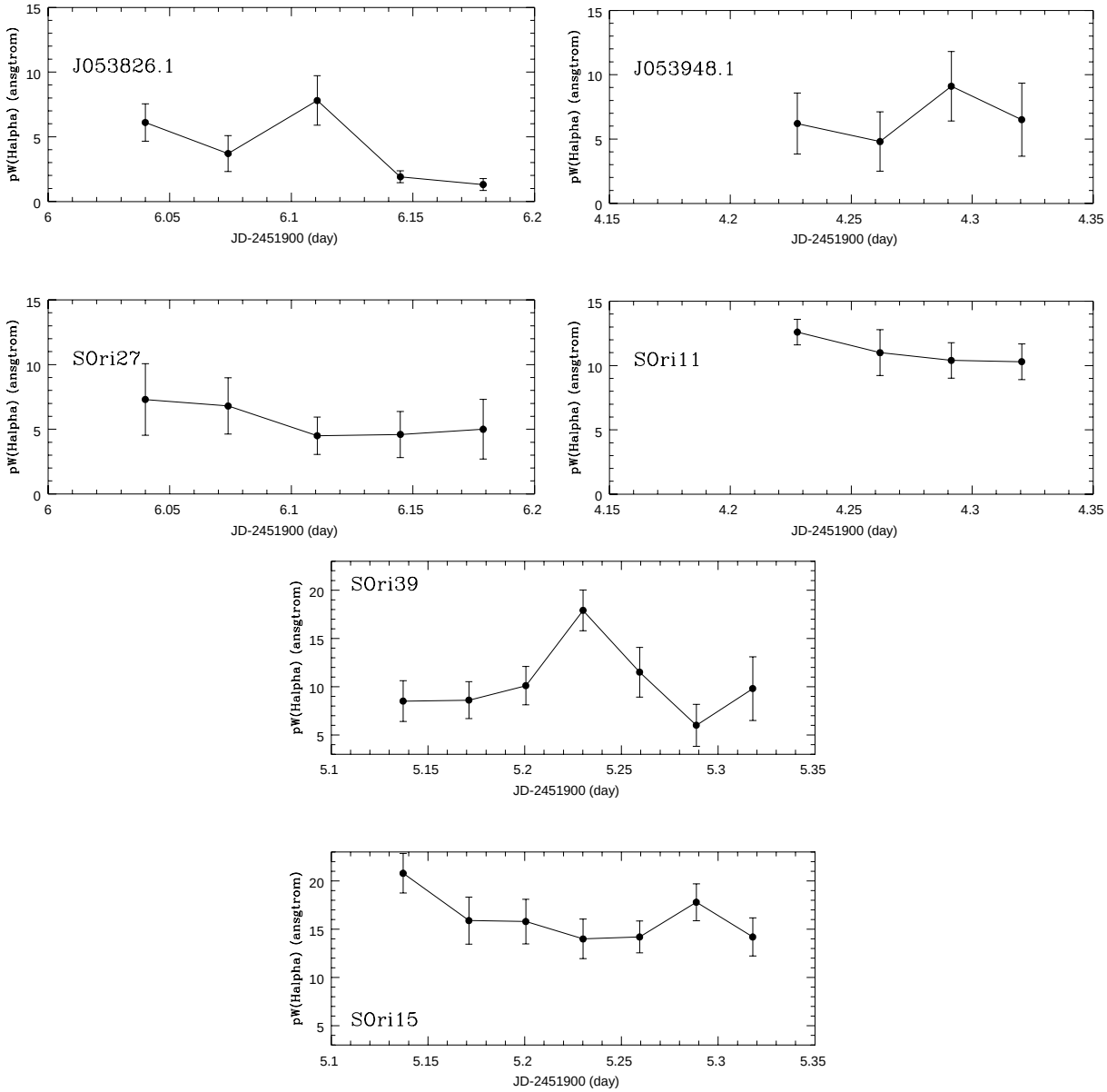

Fig. 11. Pseudo Hα equivalent with versus the Julian Date (minus 2 451 900) for several objects which have four or more independent spectra.

cases, in several objects clear differences are present, as seen in the different intensities. If our interpretation of the Hα phenomenology is correct (see previous subsection), its variability might be due to the rotation of the objects, which is the ultimate origin of the chromospheric activity via the dynamo effect (Parker 1955). Bailer-Jones & Mundt (2001), using photometric variability in the I_c filter, have measured some periodicities in several σ Orionis members (S Ori 31 and S Ori 33) and failed to find them in others (S Ori 34, 44 and 46). This periods (7.5, 8.6 hours, respectively) might correspond to the rotation of the objects. Two of them are in our survey. Unfortunately, they were only observed once. In any case, it is likely that the expected rotational periods should be in the range of few hours, whereas our exposure times were 40 min. Therefore, we should have covered a significant fraction of the phase, although the rotational periods are unknown. None but one of the BDs with large Hα emission line (SOri 38, tentatively classified as "CTT-" in Table 4) have more than one spectrum and their variability was not investigated for this reason. Figure 11 shows the Hα pseudo-equivalent widths versus the Julian Date for all objects which have at least 4 different measurements. Our time series cover about 3–4 hours, half of the rotational periods measured in young BDs belonging to the Pleiades and σ Orionis clusters. Some modulation might be present, specially in the case of S Ori 15 and S Ori 39. A photometric campaign will unveil whether, indeed, they have strong photometric variability and whether their rotational periods are in the range 2–4 hours, as the diagrams suggest.

4. Conclusions

We have collected low resolution spectroscopy of a sample of low mass stars and brown dwarfs candidate members of the σ Orionis cluster and derived spectral types by comparing with field objects. Infrared data from the 2MASS catalog was gathered for this sample and other σ Orionis candidate

members. Most of them are bona fide members of the cluster, based on the spectral type, the Hα emission and the optical and infrared photometry. The analysis of the infrared photometry indicates that a small fraction (5–12%) have *K* band excesses, a sign-post of dust disks. Moreover, by analyzing several properties (IR excess, intense Hα emission, detection of forbidden lines and lithium at 6708 Å), we have been able to classify a large number of the known low mass candidate members of the cluster either as classical or weak-line T Tauri stars. Since few of them are, indeed, of substellar nature, a more proper name would be CTT or WTT substellar analogs. Finally, we have detected spectroscopic variability (in the Hα equivalent width) for some of them. The variability timespan is compatible with the expected rotational period of this type of objects.

Acknowledgements. We thank the ESO staff at Paranal Observatory and appreciate the excellent suggestions by the referee, Xavier Delfosse. Partial financial support was provided by the Spanish This work has been partially financed by *"Programa Ramón y Cajal"* and AYA2001-1124-CO2 programs. EM acknowledges support from National Aeronautics and Space Administration (NASA) grant NAG5-9992 and National Science Foundation (NSF) grant AST-0205862. This research has made use of the NASA/IPAC Infrared Science Archive, which is operated by the Jet Propulsion Laboratory, California Institute of Technology, under contract with NASA.

References

Alcalá, J. M., & Chavarría, K. C., & Terranegra, L. 1996, A&A, 330, 1017
Apai, D., Pacucci, I., Henning, Th., et al. 2002, ApJ, 573, 115
Appenzeller, I., & Mundt, R. 1989, A&A Rev., 1, 291
Bailer-Jones, C. A. L., & Mundt, R. 2001, A&A, 3674, 1071
Baraffe, I., Chabrier, G., Allard, F., & Hauschildt, P. H. 1998, A&A, 337, 403
Baraffe, I., Chabrier, G., Allard, F., & Hauschildt, P. H. 2002, A&A, 382, 563
Barrado y Navascués, Lapatero Gsorio, M. R., Béjar, V. J. S., et al. 2001, A&A, 377, 9
Barrado y Navascués, Lapatero Gsorio, M. R., Martin, E. L., et al. 2002a, A&A, 393, 85
Barrado y Navascués, et al. 2003, in preparation
Basri, G., Mohanty, S., Allard, F., et al. 2000, ApJ, 538, 363
Bate, M. R. 2002, in The origins of Stars and Planets: the VLT view, ed. J. Alves, & M. McCaughrean (Springer-Verlag series ESO Astrophysics Symp.), 139
Béjar, V. J. S., Zapatero Osorio, M. R., & Rebolo, R. 1999, ApJ, 521, 671
Béjar, V. J. S., Martín, E. L., Zapatero Osorio, M. R., et al. 2001, ApJ, 556, 830
Bertout, C. 1989, ARA&A, 27, 351
Bessell, M. S., & Brett, J. M. 1988, PASP, 100, 1134
Bessell, M. S. 1991, AJ, 101, 662
Bodenheimer, P. 1998, in Brown Dwarfs and Extrasolar Planets, ed. R. Rebolo, E. L. Martín, & M. R. Zapatero Osorio (San Francisco: ASP), ASP Conf. Ser., 134, 115
Boss, A. P. 2001, ApJ, 551, L167
Brown, A. G. A, de Geus, E. J., & de Zeew, P. T. 1994, A&A, 289, 101
Burrows, A., et al. 1997, ApJ, 491, 856
Camenzind, M. 1990, Rev. Mod. Astron., 3, 234
Chabrier, G., Baraffe, I., Allard, F., & Hauschildt, P. 2000, ApJ, 542, L119
D'Antona, F., & Mazzitelli, I. 1994, ApJS, 90, 467
D'Antona, F., & Mazzitelli, I. 1997, in Cool Stars in Clusters and Associations, ed. R. Pallavicini, & G. Micela, Mem. Soc. Astron. It., 68(4), 807
Fernández, M., & Comerón, F. 2001, A&A, 380, 264
Garrison, R. F. 1967, PASP, 79, 433
Gershberg, R. E., Katsova, M. M., Lovkaya, M. N., Terebizh, A. V., & Shakhovskaya, N. I. 1999, A&AS, 139, 555
Gizis, J. E., Monet, D. G., Reid, I. N., et al. 2000, AJ, 120, 1085
Hawley, S. L., Gizis, J. E., & Reid, I. N. 1996, AJ, 112, 2799
Herbig, G. H., & Bell, K. R. 1988, Lick Observatory Bulletin, Lick Observatory
Herbst, W., & Miller, J. R. 1989, AJ, 97, 891
Hodgkin, S. T., Jameson, R. F., & Steele, I. A. 1995, MNRAS, 274, 869
Jayawardhana, R., Ardila, D. R., & Stelzer, B. 2002, in Brown Dwarfs, IAU Symp., 211, ed. E. L. Martín, ASP Conf. Ser., in press
Jameson, R., et al. 2002, in Brown Dwarfs, IAU Symp., 211, ed. E. L. Martín, ASP Conf. Ser., in press
Kenyon, M. J., Jeffries, R. D., & Naylor, T. 2003, in Cool Stars, Stellar Systems and the Sun 12th, ed. A. Brown, T. R. Ayres, & G. M. Harper [astro-ph/0109099]
Kirkpatrick, D., Reid, I. N., Liebert, J., et al. 1999, ApJ, 519, 802
Kirkpatrick, J. D., Reid, I. N., Liebert, J., et al. 2000, AJ, 120, 447
Kumar, S. S. 1963, ApJ, 137, 1121
Lada, C. J., Lada, E. A., Muench, A. A., Haisch, K. E., & Alves, J. 2002, in The origins of Stars and Planets: the VLT view, ed. J. Alves, & M. McCaughrean (Springer-Verlag series ESO Astrophysics Symp.), 155
Lee, T. A. 1968, ApJ, 152, 913
Luhman, K. L. 1999, ApJ, 525, 466
Luhman, K. L. 2000, ApJ, 544, 1044
Luhman, K. L., Briceño, C., Stauffer, J. R., et al. 2003, AJ, in press
Lyngå, G. 1981, Catalog of Open Star Clusters, Astronomical Data Center Bulletin V.1, 90
Lyngå, G. 1987, Catalog of Open Cluster Data, 5th ed. (Lund: Lund Obs.)
Martín, E. L. 1997, A&A, 321, 492
Martín, E. L., Delfosse, X., Basri, G., et al. 1999, AJ, 118, 2466
Martín, E. L., Zapatero Osorio, M. R., Barrado y Navascués, D., Béjar, V. J. S., & Rebolo, R. 2001, ApJ, 558, 117
Meyer, M. R., Calvet, N., & Hillenbrand, L. A. 1997, AJ, 114, 288
Muench, A. A., Alves, J., Lada, C. J., & Lada, E. A. 2001, ApJ, 558, L51
Muzerolle, J., Briceño, C., Calvet, N., et al. 2000, ApJ, 545, L141
Natta, A., & Testi, L. 2001, A&A, 376, 22
Natta, A., Testi, L., Comerón, F., et al. 2002, A&A, 393, 597
Oliveira, J. M., Jeffries, R. D., Kenyon, M. J., Thompson, S. A., & Naylor, T. 2002, A&A, 382, L22
Pickett, B. K., Durisen, R. H., Cassen, P., & Mejia, A. C. 2000, ApJ, 540, 95
Parker, E. N. 1955, ApJ, 122, 293
Rieke, G. H., & Lebofsky, M. J. 1985, ApJ, 288, 618
Reipurth, B. 2002, in The origins of Stars and Planets: the VLT view, ed. J. Alves, & M. McCaughrean (Springer-Verlag series, ESO Astrophysics Symp.), 114
Saumon, D., Hubbard, W. B., Burrows, A., et al. 1996, ApJ, 460, 993

Skrutskie, M. F., Schneider, S. E., Stiening, R., et al. 1997, in The Impact of Large Scale Near-IR Sky Surveys, ed. F. Garzon, N. Epchtein, A. Omont, B. Burton, & P. Persi (Dordrecht: Kluwer Academic Publishing Company), 25

Stauffer, J. R., Hartmann, L. W., Prosser, C. F., et al. 1997, ApJ, 479, 776

Taylor, B. J. 1986, ApJS, 60, 577

Tej, A., Sahu, K. C., Chandrasekhar, T., & Ashok, N. M. 2002, ApJ, 578, 523

Testi, L., Natta, A., Oliva, E., et al. 2002, ApJ, 571, 155

Walter, F. M., Wolk, S. J., Freyberg, M., & Schmitt, J. H. M. M. 1997, Mem. Soc. Astron. It., 68, 1081

Wolk, S. J. 1996, Ph.D. Thesis, Univ. New York at Stony Brook

Zapatero Osorio, M. R., Béjar, V. J. S., Rebolo, R., Martín, E. L., & Basri, G. 1999, ApJ, 524, L115

Zapatero Osorio, M. R., Béjar, V. J. S., Martín, E. L., et al. 2000, Science, 290, 103

Zapatero Osorio, M. R., Béjar, V. J. S., Pavlenko, Ya., et al. 2002a, A&A, 384, 937

Zapatero Osorio, M. R., Béjar, V. J. S., Martín, E. L., Barrado y Navascués, D., & Rebolo, R. 2002b, ApJ, 569, 99

Zapatero Osorio, M. R., Béjar, V. J. S., Martín, E. L., et al. 2002c, ApJ, 578, 536